A Search for the Higgs Boson in the Four Lepton Final State

CDF note 10573

The CDF Collaboration
URL http://www-cdf.fnal.gov
(Dated: July 19, 2011)

The Higgs boson is the last undiscovered particle of the Standard Model of Particle Physics (SM). A search for SM Higgs boson decays in the four lepton final state is conducted using 8.2 fb^{-1} of data of $p\bar{p}$ collisions collected by the CDF-II detector at Fermilab's Tevatron accelerator. We reconstruct the three final states of four electrons ($4e$), four muons (4μ) and pairs of electrons and muons ($2e2\mu$) in the range 50 GeV/c^2 to 600 GeV/c^2 of the four lepton invariant mass. Our search is optimized for Higgs boson decays to Z-boson pairs but is also sensitive to the W-boson pair decay channel, where the Higgs is produced in association with a Z boson that decays to charged leptons. We expect contributions from non-resonant ZZ production and fakes of 8.9 ± 1.2 and 0.3 ± 0.1 events, respectively. In the data we observe 8 events, which is consistent with no events from Higgs boson decays, therefore we extract upper limits for the cross-section of Higgs particle production. Our most stringent limits above and below the threshold for on-shell production of ZZ are set at Higgs masses of 150 GeV/c^2 and 200 GeV/c^2 with observed cross-sections of above 15.5 and 9.3 times that of the SM ruled out at the 95% confidence level, respectively.

PACS numbers: 14.80.Bn, 11.15.Ex

I. INTRODUCTION

The vector gauge bosons mediating the weak force, the W and Z, are massive. Within the Standard Model of Particle Physics (SM) their masses arise through the combination of electroweak spontaneous symmetry breaking [1–3] (SSB) and the Higgs mechanism [4, 5]. The latter posits the presence of a scalar field and an associated particle, the as yet to be observed Higgs boson. The Higgs mechanism is also able to provide mass to the fundamental fermions through Yukawa couplings. The discovery of the Higgs boson would unambiguously confirm electroweak SSB within the SM. A SM Higgs boson with mass, M_H, below $114.4\,\mathrm{GeV}/c^2$ or with M_H between $162\,\mathrm{GeV}/c^2$ and $166\,\mathrm{GeV}/c^2$ has been excluded at the 95% confidence level in direct searches at LEP [6] and the Tevatron [7]. A recently reported [8] preliminary update of the Tevatron result has expanded this 95% exclusion range to values of M_H between 158 and $173\,\mathrm{GeV}/c^2$. At the Tevatron, production of the Higgs boson can proceed either via gluon-gluon fusion (ggH), massive vector boson fusion (VBF) or associated production (WH or ZH).

In this Letter we report on the search for the Higgs boson via processes that yield four electrons ($4e$), four muons (4μ) or two electrons and two muons ($2e2\mu$) in the final state using data of $p\bar{p}$ collisions at center of mass energy 1.96 TeV collected with the CDF II detector [9], corresponding to $8.2\,\mathrm{fb}^{-1}$ of integrated luminosity . This final state configuration is dominated by the Higgs decay to a pair of Z bosons which in turn subsequently decay to charged leptons, for which our analysis is optimized as we conduct a search for the signal in the spectrum of the four lepton invariant mass ($4l$). Along with ggH and VBF our search is sensitive to associated Higgs production processes, where the accompanying boson decays hadronically or invisibly. We are also sensitive to the Higgs decay to W boson pairs, which in turn decay into muons and electrons, where the Higgs boson is produced in association with a Z boson that decays to charged leptons. Although the $4l$ invariant mass is not ideal for examining this final state our sensitivity is improved owing to the large branching fraction of the Higgs to the W boson pair decay channel.

The detection of four leptons offers one of the cleanest signatures available for analysis at a hadron collider due to the small probability of jets to produce fake lepton candidates. The requirement of four isolated identified leptons renders background from ubiquitous multi-jet processes negligible. Our analysis implements a minimal set of criteria that ensure four well reconstructed leptons only requiring, as mentioned previously, same flavour requirements on lepton pairs.

II. DETECTOR DESCRIPTION

The CDF II detector consists of a solenoidal spectrometer with a silicon tracker and an open cell drift-chamber (COT) surrounded by calorimeters and muon detectors [9]. The geometry is characterized using the azimuthal angle ϕ and the pseudorapidity $\eta \equiv ln[\tan(\theta/2)]$, where θ is the polar angle relative to the proton beam axis. Transverse energy, E_T, is defined to be $E\sin\theta$, where E is the energy of an electromagnetic (EM) and hadronic calorimeter energy cluster. Transverse momentum, p_T, is the track momentum component transverse to the beam line. The most precise tracking and calorimetry is available in the central region, ($|\eta| \leq 1.1$). There is additional but less precise detection in the forward region, ($1.2 \leq |\eta| \leq 2.0$). Calorimetry but not tracking extends out into the far forward regions ($2.0 \leq |\eta| \leq 2.8$).

III. SELECTION

We perform this search events are triggered and leptons reconstructed in the same way as it's done in the search for H→WW→ $\ell\nu\ell\nu$ at CDF[7].

This analysis uses physics objects identified as electron and muon candidates, which are referred to as electrons and muons for simplicity. In general electrons are detected by matching a central or forward track to energy deposited in the calorimeter while muons are detected by matching a central or forward track to the lack of a deposit, with or without associated stubs in the various muon chambers beyond the calorimeters. Taus are considered too difficult to detect to include in this search, except indirectly as they decay to electrons or muons in flight.

Candidate leptons are separated into eleven categories: three for electrons; seven for muons; and one for isolated tracks that project to detector regions with insufficient calorimeter coverage for energy measurements, the latter are denoted IsoTrk. The electron categories are distinguished by whether the electron is found in the central region, either a tight central electron (TCE) or likelihood-based electron (LBE), or in the forward calorimeter ($|\eta| > 1.1$) where silicon-only tracking is available, denoted a phoenix electron (PHX). LBE candidates rely on a likelihood selection that is based on track quality, track-calorimeter matching, calorimeter energy, calorimeter profile shape, and isolation information. Five of the muon catecories rely on direct detection in the muon chambers. These include categories denoted CMUP, CMP, CMX, CMXMsKs and BMU. CMUP and CMP candidates use the central muon detector

($|\eta| < 0.65$). CMX and CMXMsKs candidates use the central muon extension detector ($0.65 < |\eta| < 1.0$). BMU candiates use the intermediate muon detector ($1.0 < |\eta| < 1.5$). The remaining two categories, denoted CMIOCES and CMIOPES, rely on track matches to minimum ionization deposits in the central and forward electromagnetic calorimeters respectively. All leptons are required to be isolated by imposing the condition that the sum of the transverse energy of the calorimeter towers in a cone of $\Delta R = \sqrt{(\Delta\phi)^2 + (\Delta\eta)^2}$ equal to 0.4 around the lepton have less than 10% of the electron E_T (muon p_T).

The probability that a jet will be misidentified as a lepton is measured using samples of jet data collected using four dfferent jet E_T trigger thresholds (20, 50 , 70 and 100 GeV) and corrected for the contributions of leptons from W and Z boson decays. The range of measured fake rates for the lepton categories, which vary according to E_T or p_T are: $1\% - 3\%$ TCE, $0.5\% - 1.5\%$ LBE, $2\% - 6\%$ PHX, $0.5\% - 3\%$ CMUP, $2\% - 4\%$ CMP, $0.5\% - 2\%$ CMX, $1\% - 3\%$ CMXMsKs, $0.5\% - 2\%$ BMU, $0.5\% - 1.5\%$ CMIOCES, $2\% - 6\%$ CMIOPES, and $0.5\% - 3\%$ IsoTrk.

Each of the events analyzed is selected by a trigger, which performs real time selection of high-E_T electrons or high-p_T muons. One electron trigger requires an EM energy cluster in the central calorimeter with transverse energy greater than 18 GeV pointed to by a COT track with transverse momentum greater than 8 GeV. Muon triggers are based on track segments in the muon chambers that are matched to a COT track with transverse momentum greater than 18 GeV. Trigger efficiencies are measured using samples of observed leptonic Z decays [9]. The lepton matched to the trigger lepton must have transverse energy (momemtum) greater than 20 GeV for electrons (muons). Additional charged leptons are required to have transverse energy (momentum) greater than 10 GeV. We require exactly four leptons, where each must be separated from any other by a minimum ΔR of 0.1. This analysis evolved from the CDF measurement of the ZZ production cross-section in the four lepton final state, where constraints on the invariant mass of opposite sign same flavor dilepton pairs are imposed in order to explicitly reconstruct Z bosons [10]. For Higgs masses less than $180\,\mathrm{GeV}/c^2$ one of the Z bosons is guaranteed to be off-shell, as such requirements on the mass becomes inefficient. Nominally the mass constraints for dilepton pairs masses are above $20\,\mathrm{GeV}/c^2$ and below $140\,\mathrm{GeV}/c^2$. In the all same flavor final state opposite charge pairings are assigned on the basis of the separation from the Particle Data Group mass for the Z-boson. Given the smallness of backgrounds we found having no explicit constraint on the mass improves our sensitivity to $H \to ZZ$. The Higgs boson signature can also involve jets of hadrons produced from the decay of one of associated vector boson in the ZH or WH process, forward quarks in the VBF process, or from the radiation of gluons. We place no restriction on the number of jets allowed in the event.

IV. SAMPLES AND BACKGROUND ESTIMATION

The selected events consist primarily of the background from non-resonant diboson production of Z-boson pairs (ZZ). To a much smaller extent we suffer from mis-reconstructed ZZ events and from $Z\gamma$ production in association with jets, both of which contribute with signatures of three or two real leptons with one or two fake leptons from jets and/or the photon. The background from top-anti-top production is found to be negligible.

The acceptances, efficiencies and kinematic properties of the signal and background processes are determined primarily using simulation. Events are simulated with PYTHIA[11] for Higgs processes $gg/\mathrm{VBF} \to H \to Z^{(*)}Z^{(*)}$, associated production $(W/Z)H \to (W/Z)Z^{(*)}Z^{(*)}$, $ZH \to ZWW$ and non-resonant diboson ZZ production. A $Z\gamma$ sample is simulated according to the process described in [12]. CTEQ5L parton distribution functions (PDFs) are used to model the momentum distribution of the initial-state partons [13].

The cross sections for each process are normalized to: next-to-next leading order (NNLO) calculations with logarithmic resummation (ggH [14, 15]), NNLO (VH [16–18]), and next-to-leading order calculations (VBF [16, 19], ZZ [20], and $Z\gamma$ [21]).

The response of the CDF II detector is modelled with a GEANT-based simulation [22]. Efficiency corrections for the simulated CDF II detector response for leptons and photon conversions are determined using samples of observed $Z \to ll$ and photon conversions respectively. A correction to the simulated track resolution is applied, which is obtained from a fit to the dimuon invariant mass in the Z peak.

To estimate the total contribution from fakes in data we reconstruct events with two or three leptons and additional jets that are prone to faking leptons and weight these events with the measured jet to lepton fake rate probabilities. This method yields a very small number of events that pass the selection (as expected). These are too few to form a reasonable kinematic distribution in the four lepton invariant mass, which we model using a weighted sum of the distributions derived from the ZZ and $Z\gamma$ MC samples. The kinematic distribution of the component of fakes from badly reconstructed ZZ is assumed to be the same as that of correctly reconstructed ZZ events.

We apply the same procedure to the $Z\gamma$ MC sample to obtain the invariant mass distribution for the remaining background component. This is found to be well modeled by a Landau function. In summary the overall normalization of the estimated fake background is derived using the data-driven approach while the shape of the distribution is derived from MC.

TABLE I: The expected and observed limits of the Higgs production cross section normalised to the SM prediction for Higgs masses from 120 GeV to 300 GeV in steps of 10 GeV.

H→ 4ℓ	120	130	140	150	160	170	180	190	200	210	220	230	240	250	260	270	280	290	300
$-2\sigma/\sigma_{SM}$	58.0	21.5	12.4	10.0	15.9	24.4	18.1	7.1	7.6	9.4	10.2	12.2	12.7	14.6	16.3	18.3	19.2	21.7	23.0
$-1\sigma/\sigma_{SM}$	67.0	23.9	13.2	10.9	18.0	30.9	19.9	8.3	9.7	11.1	12.3	13.9	15.0	17.5	19.0	20.9	20.8	24.0	26.0
Median/σ_{SM}	**82.8**	**27.2**	**15.6**	**12.8**	**23.3**	**40.2**	**26.2**	**11.1**	**12.9**	**14.9**	**16.6**	**17.8**	**19.4**	**23.0**	**25.4**	**26.6**	**26.3**	**32.0**	**34.6**
$+1\sigma/\sigma_{SM}$	111.2	38.0	21.0	17.0	30.6	55.7	37.4	14.8	17.4	21.1	23.5	25.3	27.4	32.9	36.0	38.0	37.2	46.3	45.6
$+2\sigma/\sigma_{SM}$	149.3	49.9	31.1	24.2	43.3	73.2	47.4	21.7	22.0	29.8	37.8	36.4	38.9	43.1	47.7	54.1	49.5	63.1	64.6
Observed/σ_{SM}	**101.7**	**35.1**	**21.6**	**15.5**	**28.5**	**46.4**	**21.9**	**11.6**	**9.3**	**9.5**	**12.1**	**21.3**	**20.1**	**18.3**	**19.0**	**20.1**	**21.6**	**29.1**	**33.3**

Based on the selection described above in the range of the four lepton invariant mass from $50\,\mathrm{GeV}/c^2$ to $600\,\mathrm{GeV}/c^2$ we expect 8.9 ± 1.2 ZZ and 0.3 ± 0.1 fake events. For a SM Higgs mass of 150 GeV we expect conributions of: 0.20 (ggH), 0.02 (VBF), 0.02 (WH), and 0.01 (ZH) yielding a total of 0.25 ± 0.03 events. The indicated uncertainties are statistical and systematic that are combined in quadrature. The latter are described below.

V. RESULTS

In data we observe a total of 8 events, which is consistent with no excess that could be assigned to Higgs Boson decays. The four lepton invariant mass distribution is plotted in Figure 1 overlayed with expected contributions from the different background and the Higgs contribution for a mass of $150\,\mathrm{GeV}/c^2$. To cross check our result we examined the distribution in data of the magnitude of the missing transverse energy vector [34] and the number of jets. Both were found to be consistent with that expected from ZZ production.

We set upper limits at the 95% confidence level (C.L.) on the Higgs production cross section, σ_H, expressed as a ratio to the expected SM rate as a function of m_H . We employ a Bayesian technique [23] using a likelihood function constructed from the joint Poisson probability of observing the data in each bin of the four-lepton invariant mass variable, integrating over the uncertainties of the normalization parameters using Gaussian priors. A constant prior in the signal rate is assumed. The expected limit and associated one and two sigma bands are given along with the observed limit in Table I and Fig. 2.

The most stringent limit, σ_H less than $11.1 \times \sigma_{SM}$, is expected for m_H =190 GeV/c^2, while the best observed limit is σ_H less than $9.3 \times \sigma_{SM}$ for m_H =200 GeV/c^2. Owing to no direct mass constraints on the dilepton systems, we find at the intermediate Higgs mass (m_H=150 GeV/c^2) that we have a comparable sensitivity, with an expected (observed) limit of σ_H less than 12.8 (15.5) $\times\sigma_{SM}$ at the 95% C.L. [**?**]

VI. SYSTEMATIC UNCERTAINTIES

When setting these limits we consider a variety of possible systematic effects including both those that change the normalization and the shape of the kinematic distributions. The dominant systematic uncertainties are those on the theory predictions for the cross sections of signal and background processes. Systematic uncertainties associated with the Monte Carlo simulation affect the Higgs, ZZ and $Z\gamma$ acceptances taken from the simulated event samples.

Uncertainties originating from the lepton selection and trigger efficiency measurements are propagated through the acceptance calculation leading to uncertainies of 3.6% and 0.5%, respectively, on the predicted signal and background event yields. In addition, all signal and background estimates obtained from simulation have an additional 5.9% uncertainty originating from the measurement of the luminosity [24]. The $gg \to H$ cross-section has been computed at next-to-next leading order (NNLO) and next-to-next leading log (NNLL) precision with the associated scale and PDF α_s variations [25–27]. We apply a systematic uncertainty of 7% and 7.7% for the scale and PDF+α_s variations, respectively. These are equivalent to the uncertainties applied in the CDF $H \to WW$ search [28] that used 7.1fb^{-1} of data. Uncertainties from VBF and associated Higgs production channels, which account for about a quarter of the total Higgs events are assigned uncertainties of 5% and 10%, respectively, according to the recommendation of the TeV4LHC working group [29]. A 3% uncertainty is assigned on the branching fraction of Higgs to ZZ and WW, which are 100% correlated [29]. The Pythia ZZ production Monte Carlo used for acceptances and efficiency determination is at LO; using MCFM[30] we calculated the difference in the acceptance due to a full NLO simulation and found it to be ±2.5%, which is assigned as a systematic uncertainty. We assign a 10% uncertainty on the ZZ cross-section based on the difference of predictions between LO and NLO [31]. For the Zγ spectrum in the four lepton invariant mass

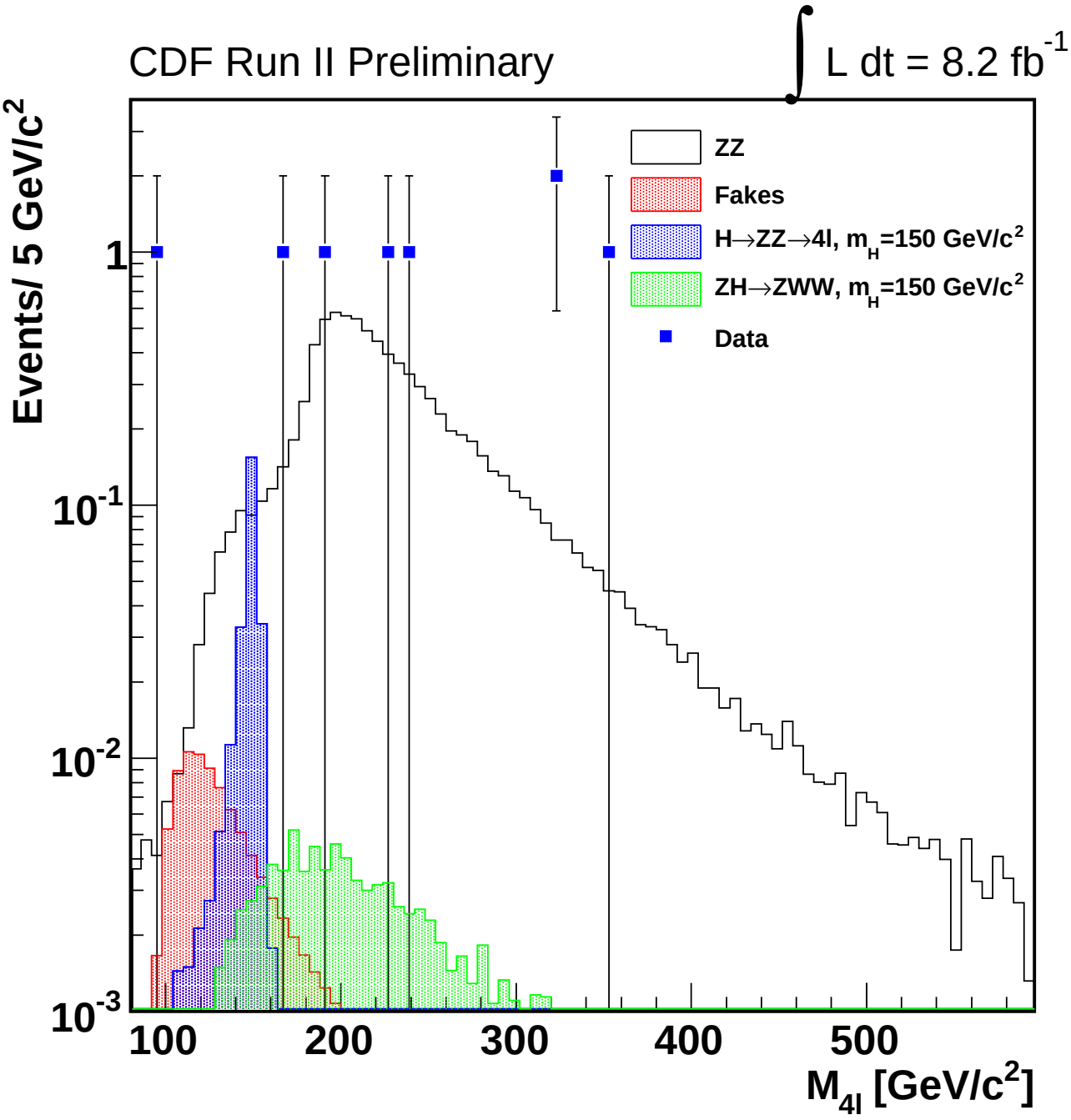

FIG. 1: The distribution of the four-lepton invariant mass as measured in data. Overlayed are estimated contributions from non-resonant ZZ production, fakes component, and from the $H \to ZZ$ and $ZH \to ZWW$ four-lepton final state for a Higgs mass of 150 GeV/c^2.

we assign an uncorrelated 50% uncertainty on the yield in each bin to account for potential mis-modelling from the use of the Landau function to model the shape. We measure the fake rates in several jet samples and we consider the maximum spread between these measurements as a systematic uncertainty on the background estimation. Propagated through to the acceptance this results in a 50% variation in the fakes yield. A summary is given in Tab II.

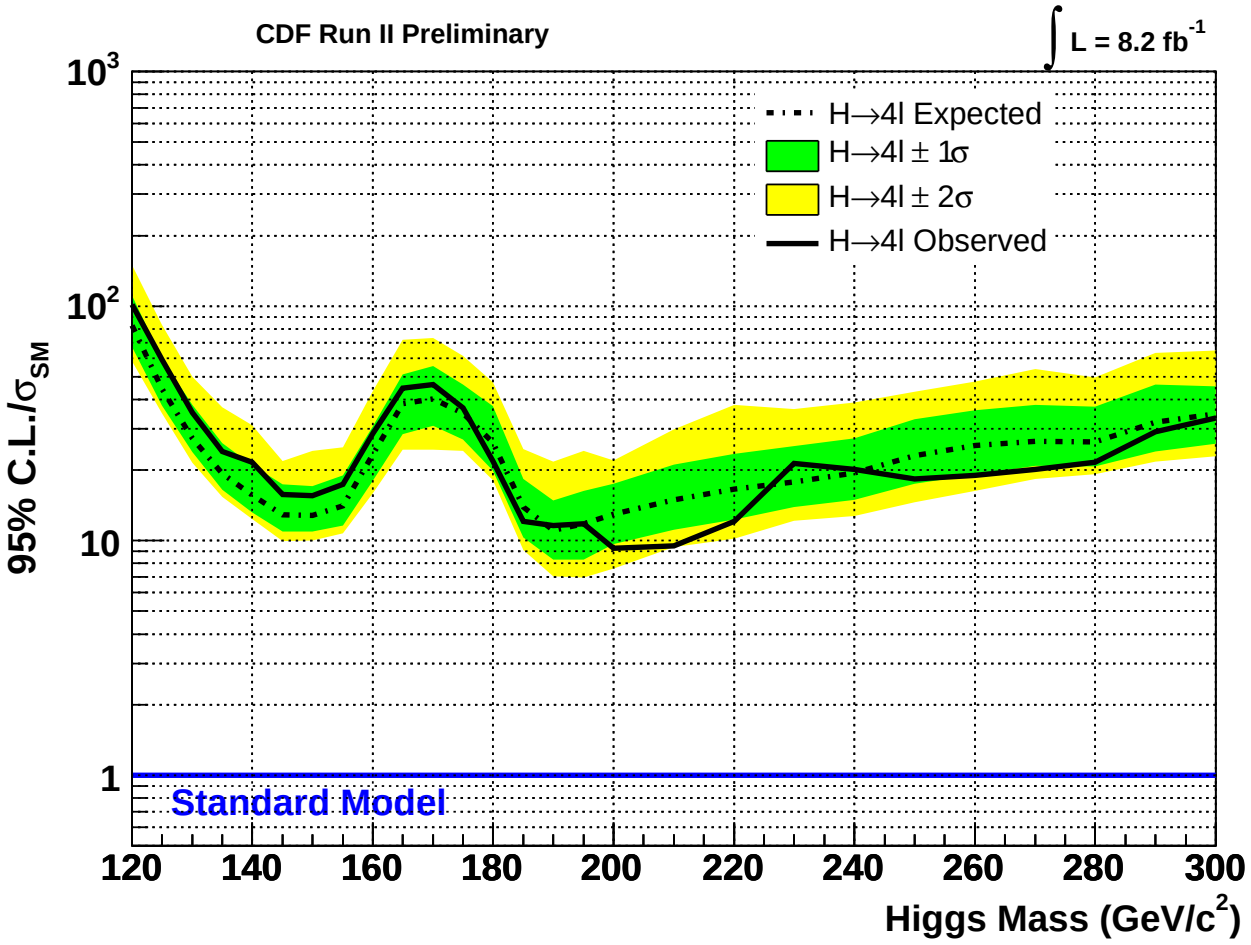

FIG. 2: The expected and observed limits of the Higgs production cross section normalised to the SM prediction as a function of the Higgs mass as derived from the search in the four lepton final state.

TABLE II: Summary of the variations considered in the evaluation of systematic uncertainty on the limit extraction

Uncertainty Source	ZZ	$Z(\gamma^*)$	gg→H	WH	ZH	VBF
Cross Section						
Scale			7.0%			
PDF			7.7%			
Total	10%			5%	5%	10%
$\mathcal{BR}$(H→VV)			3%	3%	3%	3%
Acceptance						
Higher-order Diagrams	2.5%					
PDF	2.7%					
Luminosity	5.9%		5.9%	5.9%	5.9%	5.9%
Lepton ID Efficiencies	3.6%		3.6%	3.6%	3.6%	3.6%
Trigger Efficiencies	0.4%		0.5%	0.5%	0.5%	0.5%
Fake Rates		50%				

VII. CONCLUSIONS

In 8.2fb^{-1} of data we see no evidence, as expected, for a Higgs boson in the mass range 100 GeV/c^2 to 300 GeV/c^2. We set the first limit on the Higgs production cross section in the inclusive four lepton final state, exploiting the best current sensitivity not only in the high mass region where both Z's are produced on-shell but also in the lower mass

region at the mass of around $150\,\mathrm{GeV}/c^2$.

[1] Y. Nambu and G. Jona-Lasinio, Phys. Rev. **122**, 345 (1961).
[2] Y. Nambu and G. Jona-Lasinio, Phys. Rev. **124**, 246 (1961).
[3] Y. Nambu, Int. J. Mod. Phys. **A24**, 2371 (2009).
[4] P. W. Higgs, Phys. Lett. **12**, 132 (1964).
[5] P. W. Higgs, Phys. Rev. Lett. **13**, 508 (1964).
[6] R. Barate et al. (LEP Working Group for Higgs boson searches), Phys. Lett. **B565**, 61 (2003).
[7] T. Aaltonen et al. (CDF and D0), Phys. Rev. Lett. **104**, 061802 (2010).
[8] T. Aaltonen et al. (CDF and D0) (2011), 1103.3233.
[9] A. Abulencia et al. (CDF Collaboration), J.Phys.G **G34**, 2457 (2007).
[10] M. Bauce, *et al.* (CDF Collaboration) (2009), CDF/PHYS/ELECTROWEAK/PUB/9910.
[11] T. Sjostrand, S. Mrenna, and P. Skands, JHEP **05**, 026 (2006).
[12] U. Baur and E. L. Berger, Phys. Rev. **D47**, 4889 (1993).
[13] H. L. Lai *et al.* (CTEQ), Eur. Phys. J. **C12**, 375 (2000).
[14] D. de Florian and M. Grazzini, Phys. Lett. **B674**, 291 (2009).
[15] C. Anastasiou, R. Boughezal, and F. Petriello, JHEP **04**, 003 (2009).
[16] K. Assamagan et al. (Higgs Working Group Collaboration), pp. 1–169 (2004), hep-ph/0406152.
[17] O. Brein, A. Djouadi, and R. Harlander, Phys. Lett. **B579**, 149 (2004).
[18] M. L. Ciccolini, S. Dittmaier, and M. Kramer, Phys. Rev. **D68**, 073003 (2003).
[19] E. L. Berger and J. M. Campbell, Phys. Rev. **D70**, 073011 (2004).
[20] J. Campbell and R. K. Ellis, Phys. Rev. **D60**, 113006 (1999).
[21] U. Baur, T. Han, and J. Ohnemus, Phys. Rev. **D57**, 2823 (1998).
[22] R. Brun, R. Hagelberg, M. Hansroul, and J. Lassalle, CERN-DD-78-2-REV and CERN-DD-78-2.
[23] K. Nakamura et al. (Particle Data Group), J.Phys.G **G37**, 075021 (2010).
[24] D. Acosta *et al.*, Nucl. Instrum. Meth. **A494**, 57 (2002).
[25] M. Grazzini, *Hnnlo*, http://theory..infn.it/grazzini/codes.html.
[26] S. Catani and M. Grazzini, Phys.Rev.Lett. **98**, 222002 (2007).
[27] M. Grazzini, JHEP **0802**, 043 (2008).
[28] e. a. T. Aaltonen, *Cdf search for higgs to ww* production using a combined matrix element and neural network technique*, http://www-cdf.fnal.gov/physics/new/hdg/Results.html.
[29] TeV4LHC, *Standard model higgs cross sections at hadron colliders*, http://maltoni.home.cern.ch/maltoni/TeV4LHC/SM.html.
[30] J. Campbell, K. Ellis, and C. Williams, *Monte carlo for femtobarn processes*, http://mcfm.fnal.gov/mcfm.pdf.
[31] J. M. Campbell and R. K. Ellis, Phys. Rev. **D60**, 113006 (1999).
[32] P. Murat, A. Robson, and V. Giakamopoulou, *Search for High-Mass Resonances Decaying into ZZ in ppar Collisions at* $\sqrt{s}$*=1.96TeV* (2011), CDF/PUB/EXOTIC/PUBLIC/10603.
[33] The missing transverse energy vector is defined as the opposite of the vector sum of the E_T of all calorimetric towers, corrected to produce the correct average calorimeter response to jets and to muons.
[34] This result is consistent with the excess observed in the search for high-mass resonances decaying to ZZ[32]. This analysis is performed using CDF standard tracking algorithms while that uses a different one.